Numerical investigation of the secondary flow pattern in a Pelton turbine jet

Franz Josef Johann Hahn[1], Anton Maly[2], Bernhard Semlitsch[2] and Christian Bauer[2]
[1,2] Institute of Energy Systems and Thermodynamics (IET), Technische Universität Wien, Vienna, Austria
[1] franz.hahn@tuwien.ac.at

ABSTRACT

The quality of the free-surface water jet influences Pelton turbine efficiency. Secondary flows resulting from the interior parts of the injector can deform the jet shape. By numerical flow simulations, this work identifies that the secondary flow pattern in a Pelton turbine jet resembles a quadrupole potential flow. This pattern is generated by the wake formation caused by the torpedo ribs. Further, it is demonstrated how streamlining the interior parts reduces the amount of secondary flow in the jet.

Keywords: Pelton turbine injector, free-surface jet, secondary flow, quadrupole.

1 INTRODUCTION

Pelton turbines are known for their wide operating range and high part-load efficiencies. The hydraulic efficiency of the Pelton turbine is primarily governed by the interaction of the water jets with the runner buckets. Numerical (Santolin et al., 2009) and experimental studies (Staubli et al., 2009) revealed reductions over two percentage points in the turbine efficiency where a high-quality jet could not be achieved. Thus, the identification of flow features deteriorating the water jet quality is desired. According to Zhang and Casey (2007), two of these features are secondary flows in the jet and the velocity deficit in the jet core. The upstream flow history causes the secondary flows in the jet. Influences come from parts such as the torpedo, ribs, bends, and distributor pipe. These secondary flows enhance jet break-up, disturbed jet surfaces and jet core shift. The velocity deficit in the jet core results from the merging needle boundary layers. Petley et al. (2019) showed that larger needle angles reduce injector losses. However, a significant change in the secondary flow structure was not observed. The present study focuses on understanding the generation of secondary flow patterns in the jet. Numerical flow simulations of a typical injector configuration with a straight upstream pipe show how streamlining interior injector parts reduces secondary flows in the jet.

2 NUMERICAL APPROACH

Figure 1 a) displays a simplified sketch of the computational domain. It consists of the injector, a straight upstream pipe and a freestream body downstream of the nozzle. The upstream pipe has a length of three times its diameter to allow the flow to develop before entering the injector. In the freestream body the free-surface water jet is surrounded by air. Additionally, the cross-sections of the standard (upper half, red) and the streamlined rib (lower half, green) are compared. The total pressure was prescribed at the inlet equivalent to a head of 60 meters. The turbulence intensity was assumed to be 5%, and a turbulent length scale in the order of the diameter of the upstream pipe was defined. A no-slip condition was specified on all walls. The pressure was set to atmospheric conditions at the circumferential boundary of the freestream body and the outlet. To increase simulation robustness, a velocity inlet (air, 0.001 m/s) was defined at the freestream inlet. All simulations of the two-phase, steady-state flow problem were performed with the commercial solver ANSYS CFX 19.2. The two-phase nature of the flow was captured with the homogeneous model. For turbulence modelling, Menter's k-ω Shear Stress Transport model was applied. Each simulation ran for a minimum of 1500 iterations until the monitor values for flow rate and pressure remained constant for at least 500 iterations.

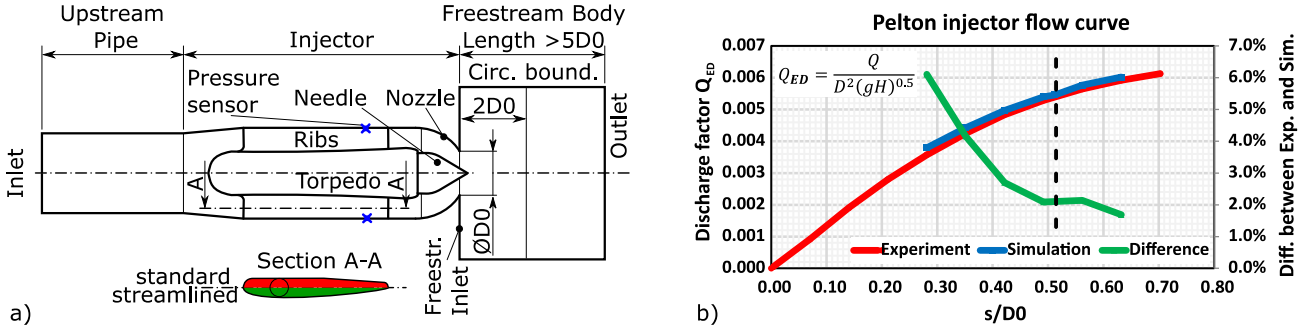

Figure 1. a) Sketch of the domain and section cut of the rib geometries, b) Comparison of simulated flow curve against experiments, where Q_{ED} defined in International Electrotechnical Commission (1999) was used.

A grid study performed for mesh sizes of 3.5, 4.9 and 6.7 million elements yielded a grid convergence index of less than 1% for the static pressure taken at the indicated sensor positions. Figure 1 b) compares the injector flow curve simulated with the medium mesh against experimental data from the laboratory test rig at IET. The simulations overestimate the discharge factor Q_{ED} in the entire operating range. This difference decreases for larger needle openings s/D_0, and the simulation approach delivers sufficient predictability.

3 RESULTS AND CONCLUSIONS

The plots of Figure 2 a) and 2 b) show that the secondary flow pattern in the jet resembles a quadrupole flow with a complex potential of $F(z) = Az^{-2}$. A possible explanation for this flow behaviour is that the wakes caused by the ribs as well as the needle boundary layer are present in the flow even after the jet exits the nozzles. In these wakes, the transport velocity is lower than outside of the wakes. To compensate the velocity deficit additional fluid from outside of the wakes is transported towards the jet core. The transport is driven by the radial pressure gradient imposed by the curvature of the nozzle. For satisfaction of continuity within a section, the fluid needs to leave the centre of the jet in a direction perpendicular to the rib wake until it is turned around close to the jet surface just to be fed to the wake again. To illustrate the effect of internals on the strength of secondary flow, the plots in Figure 2 show the difference in secondary flow for the case with standard (2a) and the case with a streamlined design (2b). Although both ribs have the same maximum thickness, the profile of the streamlined rib, which is shaped like a NACA 0012 airfoil, induces less secondary flow than the standard profile. The mass flow averaged secondary flow velocity in the investigated plane, normalised by the ideal jet velocity, $||\vec{u}_{sec}||/\sqrt{2gH}$ was reduced by 40% and the maximum value of the normalised secondary velocity decreased by over 50%. These findings lead to the conclusion that streamlining interior parts of the injector does not affect the quadrupole like structure of secondary flows in the jet, but shows great potential to reduce their magnitude.

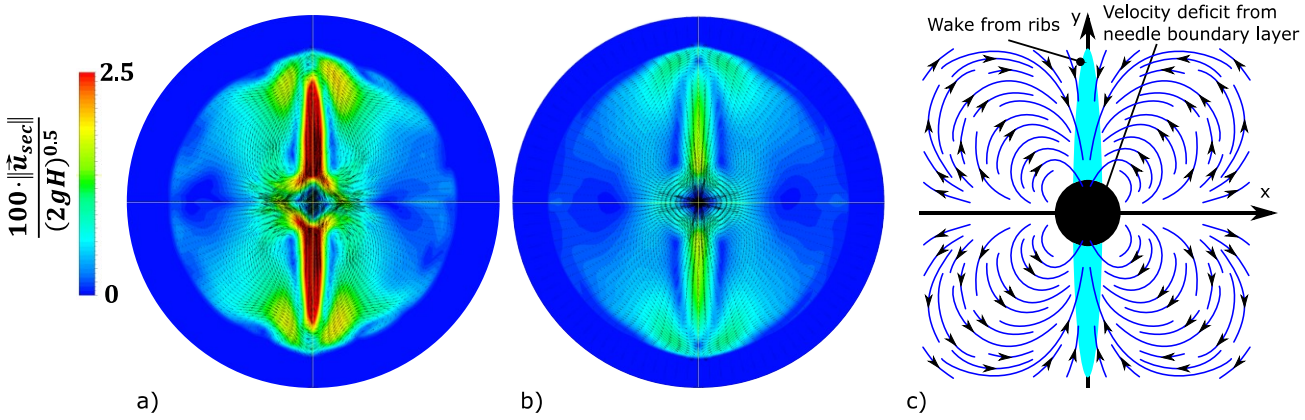

Figure 2. a) Secondary flow velocity for case (s/D_0=0.513) with standard rib at 2D0 downstream of the nozzle exit, b) same plot for case with streamlined rib and c) secondary flow pattern, shaped like a quadrupole flow.

ACKNOWLEDGEMENTS

The computational results presented have been achieved in part using the Vienna Scientific Cluster (VSC4). The authors acknowledge the financial support through the Österreichische Forschungsförderungsgesellschaft (FFG) under the project 'AxFeeder' (project number 888084).

REFERENCES

International Electrotechnical Commission. (1999). Hydraulic turbines, storage pumps and pump-turbines – Model acceptance tests (IEC 60193:1999).

Petley, S., Zidonis, A., Panagiotopoulos, A., Benzon, D., Aggidis, G.A., Anagnostopoulos, J.S., Papantonis, D.E. (2019). Out With the Old, in With the New: Pelton Hydro Turbine Performance Influence Utilizing Three Different Injector Geometries. Journal of Fluids Engineering, Vol. 141, 081103

Staubli, T., Abgottspon, A., Weibel, P., Bissel, C., Parkinson, E., Leduc, J., Leboeuf, F. (2009). Jet quality and Pelton efficiency. Proceedings of Hydro-2009, Lyon, France

Santolin, A., Cavazzini, G., Ardizzon, G., Pavesi, G. (2009), Numerical investigation of the interaction between jet and bucket in a Pelton turbine. Proceedings of the Institution of Mechanical Engineers, Part A: Journal of Power and Energy, Vol. 223, 721-728

Zhang, Zh., Casey, M. (2007). Experimental studies of the jet of a Pelton turbine. Proceedings of the Institution of Mechanical Engineers, Part A: Journal of Power and Energy, Vol. 221, 1181-1192